Proc. Natl. Acad. Sci. USA
Vol. 88, pp. 8744–8748, October 1991
Physiology/Pharmacology

Galanin inhibits a dihydropyridine-sensitive Ca^{2+} current in the RINm5f cell line

(calcium channels/insulinoma cells/whole-cell recording)

FADIA R. HOMAIDAN, GEOFFREY W. G. SHARP, AND LINDA M. NOWAK

Department of Pharmacology, College of Veterinary Medicine, Cornell University, Ithaca, NY 14853

Communicated by Robert H. Wasserman, June 24, 1991

ABSTRACT **Mechanisms of action of the neuropeptide galanin, a putative neuromodulator in the central and peripheral nervous systems, have been evaluated extensively in insulin-secreting cells isolated from pancreas and cell lines derived from pancreatic tumors. Galanin inhibits insulin secretion from these cells through several mechanisms, including activation of ATP-dependent K^+ channels and inhibition of adenylyl cyclase leading to a decrease in cAMP. Here we report that galanin also inhibits a dihydropyridine-sensitive Ca^{2+} current. Both electrophysiological actions by galanin would result in less Ca^{2+} entry, as the action to increase K^+ current would hyperpolarize the cells and the decrease in voltage-gated Ca^{2+} current would decrease Ca^{2+} influx at depolarized potentials where these channels are activated. These galanin actions would directly counter the two opposing electrophysiological responses to carbohydrate stimulation in RINm5f cells, which are to inhibit K^+ current and to stimulate Ca^{2+} current. Given that stimulation of presynaptic nerve terminals in pancreas releases galanin, these results suggest that Ca^{2+}-dependent insulin release from native pancreatic β cells may also be regulated by similar neuropeptide effects.**

Galanin-(1–29), a neuroactive peptide originally isolated from porcine intestine (1), is widely distributed throughout the vertebrate central nervous system (2). In the periphery, galanin-containing nerve terminals have been described in association with many tissues, including gut (3, 4) and pancreas (5). Galanin-mediated inhibition of insulin release has been reported *in vivo* and *in vitro* (6–10), and the quantity of galanin released by nerve stimulation was shown to be sufficient to affect pancreatic islet function (11).

Galanin appears to play an important role in the regulation of neurotransmitter and hormone release. For example, it causes inhibition of electrically or neurochemically stimulated acetylcholine release from myenteric plexus neurons (12). It also causes a decrease in bombesin-stimulated gastric acid secretion, presumably by inhibition of acetylcholine release from myenteric nerve terminals (13). In contrast to these inhibitory actions, galanin increases growth hormone and prolactin release from anterior pituitary in intact brain. However, recent studies of isolated anterior pituitary cells indicate the stimulatory actions of galanin did not occur in the absence of the hypothalamic synaptic network (14).

Previous electrophysiological studies of the mechanism of galanin regulation of hormone secretion had pointed to its action to increase K^+ conductance and hyperpolarize neuronal and secretory cells. However, intracellular recording studies also provided results suggesting that galanin may directly inhibit voltage-gated Ca^{2+} currents. In myenteric neurons galanin increased K^+ conductance and hyperpolarized the cells, but it also decreased the duration of Ca^{2+}-dependent action potentials recorded using Cs-filled pipettes (15), consistent with a direct effect on Ca^{2+} currents as well. Indirect evidence for galanin affecting Ca^{2+}-dependent currents was also reported in mudpuppy cardiac ganglia neurons where the amplitude and duration of Ca^{2+}-dependent action potentials were decreased in recordings made in tetrodotoxin and tetraethylammonium (TEA) containing solutions (16), circumstances that suggest this effect of galanin is more likely to be through inhibition of Ca^{2+} currents than through activation of K^+ currents. Again, in these parasympathetic neurons, galanin induced membrane hyperpolarization by activating K^+ conductances in the absence of TEA (16).

In this study we examined the effect of galanin on Ca^{2+} currents in RIN cells (derived from a rat insulinoma: RINm5f) using whole-cell patch-clamp recording methods. Two currents were observed with different time courses and different pharmacological properties. The early transient phase of the Ca^{2+} current was insensitive to galanin and the dihydropyridine antagonist nitrendipine, whereas the later sustained phase of Ca^{2+} current was inhibited by nitrendipine and galanin. Thus, in RIN cells galanin not only inhibits Ca^{2+} entry indirectly by activating K^+ channels (17) and hyperpolarizing them, as previously reported in a number of cell types (9, 15–18), but also directly influences dihydropyridine-sensitive Ca^{2+} channels.

MATERIALS AND METHODS

Materials. Galanin (porcine; amino acids 1–29) was obtained from Peninsula Laboratories. Roswell Park Memorial Institute medium (RPMI 1640), fetal bovine serum, streptomycin, and penicillin were purchased from GIBCO; Mg_2ATP, tetrodotoxin, and nystatin were acquired from Sigma. Nitrendipine was a gift from the Miles Institute for Preclinical Pharmacology (New Haven, CT).

Cell Culture. Cells of the insulin-secreting cell line RINm5f (RIN cells) were cultured in RPMI 1640 medium supplemented with 10% fetal bovine serum, 100 μg of streptomycin per ml, and 100 units of penicillin per ml at 37°C in a 95% air/5% CO_2 atmosphere. Cells were used 3–5 days after plating.

Patch-Clamp Recording. Whole-cell currents were typically recorded with the conventional tight-seal whole-cell configuration of the patch-clamp technique (19) at room temperature. Patch pipettes made with 7052 glass (Garner Glass, Claremont, CA) had resistances between 2 and 5 MΩ. The reference electrode was a Ag/AgCl wire placed in the bath. Currents were recorded using an LM-EPC7 patch-clamp amplifier (Medical Systems, Greenvale, NY). Stimulus protocols were generated using an Axolab system with AXESS software (Axon Instruments, Burlingame, CA), and the data were analyzed using a personal computer (IBM-AT).

The publication costs of this article were defrayed in part by page charge payment. This article must therefore be hereby marked "*advertisement*" in accordance with 18 U.S.C. §1734 solely to indicate this fact.

Abbreviations: *I–V*, current–voltage; I_p, peak inward current; I_s, sustained inward current; I_{p-s}, transient or inactivating inward current.

Experiments were performed using an extracellular (bath) solution containing (in mM) 110 NaCl, 5 CsCl, 20 $CaCl_2$, 10 sodium Hepes (pH 7.2), and 200 nM tetrodotoxin and an intracellular (pipette) solution containing (in mM) 140 CsCl, 10 EGTA/1 $CaCl_2$, 10 potassium Hepes (pH 7.2), and 4 mM Mg_2ATP. Mg_2ATP was included in pipette solutions to maintain the sustained Ca^{2+} current for 15–20 min as described (20). Control recordings in RIN cells were done for up to 20 min to demonstrate that this current did not wash out in the presence of ATP. Also, whole-cell recordings (n = 5) were performed using nystatin in the intracellular buffer to permeabilize the membrane of the cell-attached/perforated patch (21) to confirm that the inhibitory effects of dihydropyridine and galanin were observeable under conditions where the endogenous cytoplasmic factors normally maintaining a functional sustained Ca^{2+} current are less disturbed than in conventional whole-cell recordings.

The transient and the sustained inward currents appeared to be carried by Ca^{2+} ions, since both currents were insensitive to tetrodotoxin (200 nM–1 μM) and inhibited by Cd^{2+} (100–500 μM).

RESULTS

RIN Cells Contain Two Ca^{2+} Currents. Inward currents in RIN cells have been found to include voltage-activated K^+ (22, 23), Na^+ (23), and Ca^{2+} currents (24, 25). Recent reports indicate that two Ca^{2+} channel types can be observed in cell-attached patches of rat pancreatic β cells (26, 27). However, Ca^{2+} channels present in RIN cells have not been characterized as thoroughly as those in other insulin-secreting cells (28). Therefore, RIN cells were examined briefly as follows. Patch pipettes contained Cs^+ to inhibit outward K^+ currents and either 4 mM Mg_2ATP (conventional perfused whole-cell recordings) or nystatin (perforated patch method) to maintain Ca^{2+} currents. Extracellular solutions included 20 mM $CaCl_2$ to increase the size of Ca^{2+} currents and 5 mM CsCl to inhibit inwardly rectifying K^+ channels. Cells were held at −60 mV and were stimulated from either −80 or −100 mV. In most experiments, brief hyperpolarizing prepulses (to −100 mV for 100 ms) were applied to remove voltage-dependent inactivation, thus permitting the more highly sensitive transient current to be observed and allowing shorter interstimulus intervals to be used between voltage steps. Currents were evoked by long-duration (300–500 ms) depolarizing voltage steps applied in +10-mV increments so transient and sustained currents could be observed in the same cells.

Under these recording conditions, 32% of cells (22 of 69) contained a single rapidly decaying inward current (Fig. 1*A*) activated between −40 and −30 mV. This current reached a maximum amplitude near 0 mV as shown in the current–voltage (*I–V*) curve in Fig. 1A_2. Another 28% of the cells (19 of 69) also contained a single inward current; however this current decayed slowly during the stimulus pulse (Fig. 1*B*). This current also activated between −40 and −30 mV in our recording conditions, preventing it from being distinguished from the rapidly inactivating current except on a temporal basis. Thus, in whole-cell recordings the principal feature that differentiated the two currents was their time course. At the end of the stimulus pulse the slowly decaying current could still be measured, since it typically retained 70% of its maximum amplitude even at positive potentials (e.g., +20 mV) where the inactivation was more apparent (Fig. 1B_1). The two *I–V* curves in Fig. 1B_2 show that the inward current measured at the peak (I_p; ●) of each response and the sustained current (I_s; ▲) measured near the end of the stimulus reached maximum values at +20 mV, consistent with them arising from the same channels. The remaining 40% of the cells (28 of 69) (see Figs. 2 and 3) appeared to

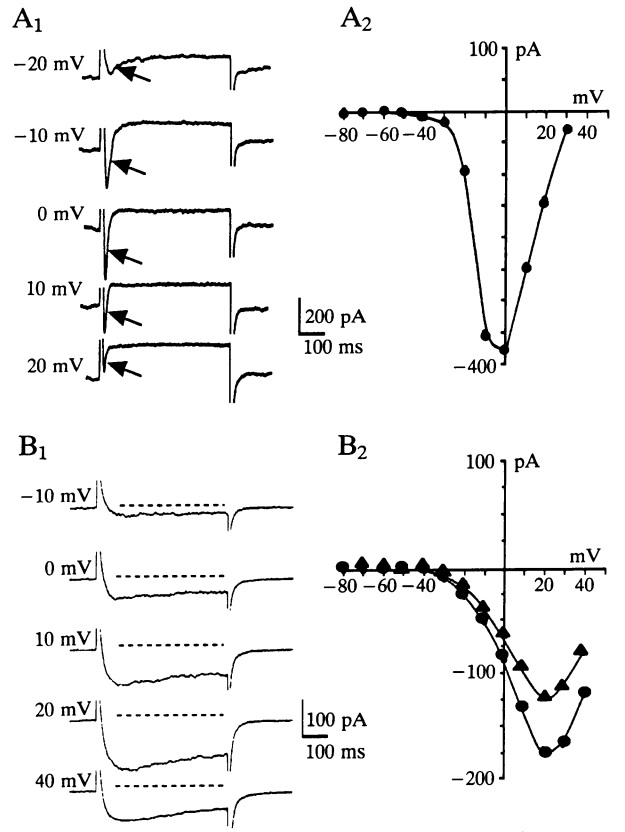

FIG. 1. (A_1) Current responses evoked by voltage steps to −20, −10, 0, 10, and 20 mV are displayed without subtracting the capacitive current transients or leak currents. Arrows indicate the rapidly inactivating inward currents. (A_2) *I–V* curve obtained for the peak (●) current at each voltage after leak current was subtracted. (B_1) Current responses evoked by voltage steps to −10, 0, 10, 20, and 40 mV are displayed without subtracting the capacitive current transients or leak currents. The magnitudes of the leak currents are indicated by the dotted lines above each trace. (B_2) Leak-subtracted *I–V* curves were obtained for the peak (●) current and for the sustained current (▲), which was measured 450 ms after the start of the pulses. Peak (I_p) and sustained (I_s) currents reached their maximum values at +20 mV. Normalizing the curves indicated they overlapped (not illustrated), suggesting that, aside from inactivation decreasing the number of effective channels, the remaining functioning channels had the same voltage-dependent probability of opening. Recordings in *A* and *B* were made using depolarizing steps (500-ms duration) applied in 10-mV increments between −80 and +30 or +40 mV. All stimuli followed a 100-ms prepulse to −100 mV that removed voltage-dependent inactivation. Cells were held at −60 mV between stimuli. Leak current was determined at potentials above −60 mV by extrapolation of the linear *I–V* curves obtained from four voltage steps from −100 to −60 mV in each recording.

contain either a mixture of both inward currents or another class of channels altogether. This latter group of cells contained inward currents with a pronounced peak and a sustained phase. The currents were initially separated from each other based upon the assumption that the current measured near the end of a long stimulus pulse represented the same sort of sustained current as illustrated in Fig. 1*B*. Thus, two phases of inward current were measured, as illustrated in the *I–V* curves of Fig. 2*B*. Two measurements were made on the raw data traces (Fig. 2*A*), one at the peak of the inward current response (within the first 50 ms) and the other taken just before the end of the stimulus pulse. The *I–V* relationships of these two measures (I_p, ○; I_s, △) suggested some differences in voltage dependence of the maximum current, with I_p reaching its greatest value at 10 mV and I_s at +20 mV in this cell. The currents were further characterized by

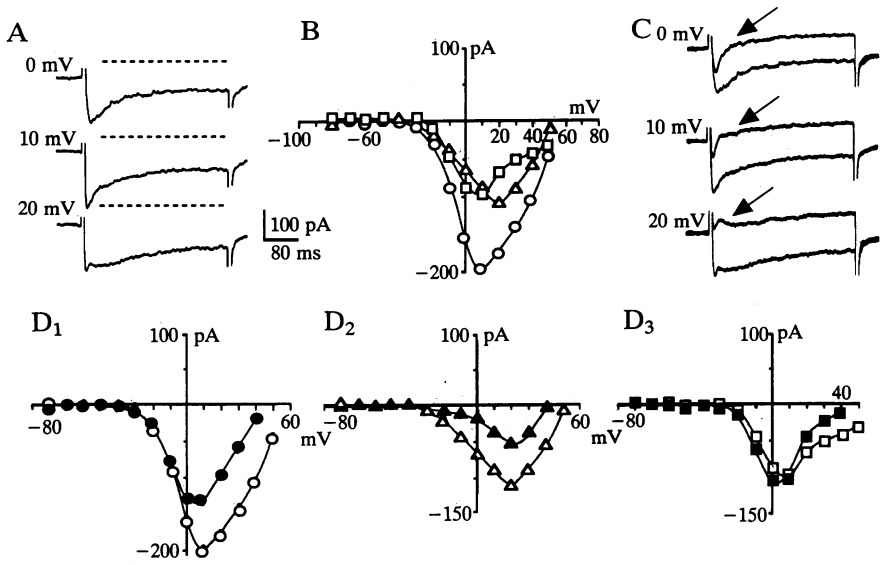

FIG. 2. Whole-cell voltage-clamp currents recorded from a RIN cell under control conditions and in the presence of nitrendipine using the perforated patch method. (*A*) Current responses evoked by voltage steps to 0, 10, and 20 mV are displayed without subtracting the capacitive current transients or leak currents. The magnitudes of the leak currents (determined by extrapolation of the linear *I–V* curves obtained from four voltage steps from −100 to −60 mV) are indicated by the dotted lines above each trace. Depolarizing steps (300-ms duration) were applied in 10-mV increments between −80 and +50 mV. The cell was held at −60 mV between stimuli. (*B*) *I–V* relationships of whole-cell currents from the recording in *A*. The peak of the inward current (I_p, ○), occurring within the first 50 ms of the onset of the depolarizing pulse, is compared to the sustained phase (I_s, △) of the current recorded near the end of the pulse (at 280 ms). Subtracting the sustained current *I–V* curve from the peak current *I–V* curve gives the third *I–V* curve (I_{p-s}, □). It has its maximum value at +20 mV and the I_{p-s} reaches its maximum between 0 and +10 mV. I_{p-s} represents the inactivating components of the rapidly and slowly inactivating currents shown in Fig. 1. (*C*) Three pairs of raw data traces show the control current (compare *A*) and the responses in nitrendipine (see arrows) at 0, 10, and +20 mV. (*D*) Pairs of *I–V* curves from the control recording (○, △, □) and in the presence of nitrendipine (●, ▲, ■) for I_p (D_1), I_s (D_2), and I_{p-s} (D_3) illustrate that the predominant effect of nitrendipine was to decrease the sustained current (D_2), which contributes substantially to the peak current in this cell (D_1). In nitrendipine the I_{p-s} current was maximum at 0 mV. A small shift to the left by the I_{p-s} curve in nitrendipine is consistent with the control I_{p-s} curve containing the inactivating components of the rapidly and slowly inactivating inward currents. Losing the contribution of the slowly inactivating current from the I_{p-s} curves in nitrendipine does not account for the current being larger between −30 and +10 mV. However, it may be due to a change in the access resistance since this often decreased over time in recordings made with nystatin. Control data were taken after the recording appeared to reach a stable series resistance (≈10 min after seal formation) and nitrendipine data were taken 3–4 min after exposure to the drug.

subtracting I_s from I_p to give a third *I–V* relationship, designated I_{p-s} (□), for each cell. The I_{p-s} current is referred to as the transient or inactivating inward current. In the 28 cells examined I_{p-s} curves always reached their maximum amplitude between 0 and +10 mV, whereas the I_s curves always reached maximum at +20 mV. This suggested that the sustained current component in this third group of cells was similar to that of the cell illustrated in Fig. 1*B*.

Several lines of evidence support the hypothesis that the two phases of current, inactivating and sustained, measured in this manner represent a combination of the two currents illustrated previously (in Fig. 1): (*i*) they reached their maximum amplitude values at slightly different voltages, (*ii*) different proportions of the two phases were observed from cell to cell, and (*iii*) the sustained phase was sensitive to washout in conventional whole-cell recording if ATP was not included in patch pipettes. Shared characteristics between the sustained current in these cells and the L-type Ca^{2+} currents in other cells (29) predicated a brief investigation of RIN cell Ca^{2+} current dihydropyridine sensitivity.

Pharmacological Differences Between Ca^{2+} Currents. The effects of the dihydropyridine antagonist nitrendipine (1 μM) on Ca^{2+} currents were examined in recordings from four cells containing currents with transient and sustained phases using either the nystatin/perforated patch method (n = 3) or conventional whole-cell recording with an ATP-containing pipette (n = 1). As shown in the data traces in Fig. 2*C* and the *I–V* curves in Fig. 2*D*, the sustained phase (I_s) of the Ca^{2+} current was highly sensitive to inhibition by nitrendipine, whereas the more transient component of the current (I_{p-s}) was relatively insensitive to this dihydropyridine. Nitrendipine (1 μM), added directly to the bath solution, inhibited the sustained Ca^{2+} current between 40% and 60% within ≈1 min of application in all four cells. Previously, 1 μM nitrendipine had been reported to cause ≈50% inhibition of the sustained Ca^{2+} current in GH3 cells (30).

Effect of Galanin on Ca^{2+} Currents. The effects of galanin on Ca^{2+} currents are illustrated in Fig. 3. In the raw data traces it is clear that 100 nM galanin substantially decreased the later phase of the inward current (Fig. 3*A*) corresponding to the sustained dihydropyridine-sensitive current. The *I–V* curves in Fig. 3 *B–D* were obtained under control conditions (open symbols) and after treatment with 100 nM galanin (filled symbols). The control *I–V* curves show the differences in the voltage sensitivity of the peak (I_p, ○), sustained (I_s, △), and transient (I_{p-s}, □) components of the inward current as previously separated in Fig. 2. Galanin caused a marked inhibition of the peak inward current at 0 mV and higher potentials (Fig. 3*B*) and markedly suppressed the sustained current in this cell (Fig. 3*C*). Again, as with nitrendipine, galanin had little effect on the more transient inward current (Fig. 3) in this cell or in any of the others examined. There was also no difference between the actions of galanin on Ca^{2+} currents in cells (n = 17) where conventional whole-cell recordings were performed compared to recordings where the nystatin-perforated patch method was used (n = 2).

Nitrendipine and galanin selectively inhibited currents in the cells exhibiting the sustained current and not in those exhibiting just the transient current.

Reversibility and Concentration Dependence of Galanin Action. Galanin (2–200 nM) inhibited the sustained Ca^{2+} current in all 23 cells examined. In a few recordings (n = 4),

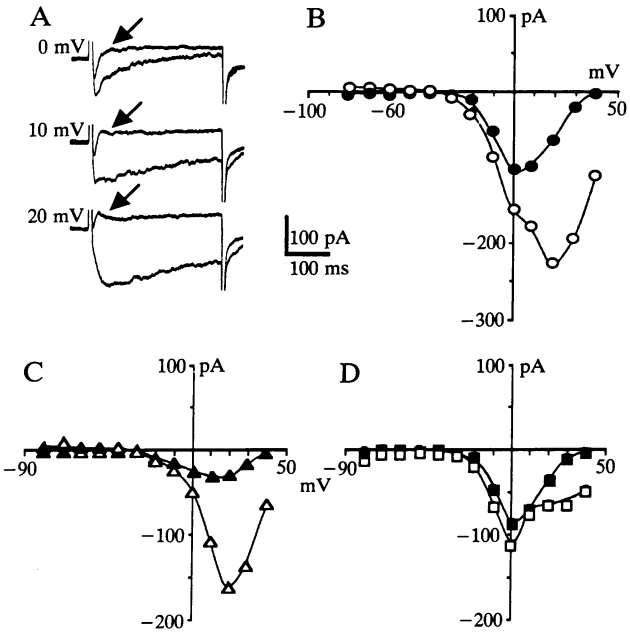

FIG. 3. Galanin inhibited the sustained Ca^{2+} current. (*A*) Pairs of raw data traces at 0, 10, and 20 mV from a recording in control (lower trace of pair) and in 100 nM galanin (arrows: upper trace of pair) indicate that galanin markedly reduced the inward current. (*B–D*) *I–V* curves were obtained from data as shown in *A* from the control (○, △, □) recording and after 4 min in galanin (●, ▲, ■). (*B*) Peak (I_p) *I–V* curve is most affected by galanin at 0 mV and above. (*C*) Sustained current (I_s) was decreased by 80% at +20 mV in this cell. It reached its maximum amplitude at +20 mV in the absence and presence of galanin. (*D*) A small decrease in the inactivating components of the current (I_{p-s}) consistent with this I_{p-s} curve also containing a contribution from the slowly inactivating current in the control solution. *I–V* curves for I_p, I_s, and I_{p-s} were obtained as described in the legend to Fig. 2*B*. Leak currents were obtained and manually subtracted as described in the legend to Fig. 1.

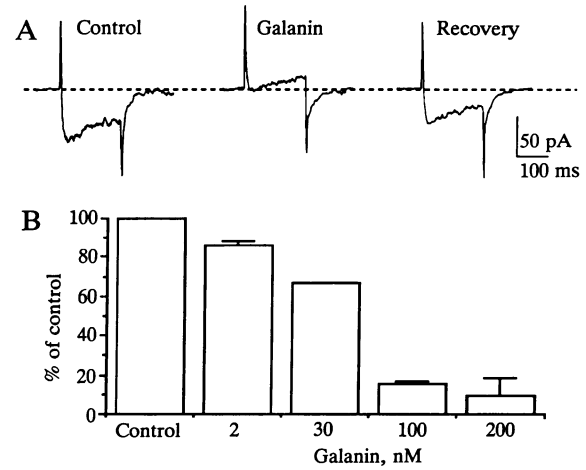

FIG. 4. (*A*) Reversibility of galanin-mediated inhibition was examined using slow bath exchange of control and galanin-containing solutions. The inward current evoked at +20 mV is displayed: in control solution (left), after addition of galanin (200 nM) to the bath solution (middle), and 4 min after beginning to wash the peptide away (right). Raw data traces are shown without subtracting capacitive transient or leak currents. The cell was held at −60 mV and repeatedly stepped to +20 mV for 200 ms at 10-s intervals to minimize inactivation. (*B*) Concentration dependence of galanin-mediated inhibition of sustained inward currents. Percent inhibition of the sustained component of inward current was determined by comparing currents measured 280 ms after the start of the stimulus pulse in control and 4 min after galanin application. The data are from 14 cells: 4 in 2 nM, 1 in 30 nM, 3 in 100 nM, and 6 in 200 nM. All responses were measured at +20 mV, where the sustained current reaches its maximum amplitude.

galanin was applied and the extracellular solution was successfully changed by slow bath perfusion to determine if galanin-mediated inhibition of Ca^{2+} currents was reversible. Results from one cell subjected to four solution changes are shown in Fig. 4*A*. The control current trace (left panel) was obtained 2 min after the beginning of the recording. Galanin inhibited the Ca^{2+} current after 1 min (Fig. 4*A*, center panel) and the current response showed partial recovery (70%) after washing with control solution for 4 min (Fig. 4*A*, right panel). A second application of galanin to this cell inhibited the Ca^{2+} current a second time, and again partial recovery was obtained after washing the cell with control medium for a second time (data not shown). Complete recovery from galanin inhibition was difficult to demonstrate because of the mechanical disturbance created by changing solutions and the apparently slow washout of the peptide.

The concentration dependence of galanin-mediated inhibition was tested using 2–200 nM galanin added by directly pipeting a concentrated galanin stock solution into culture dishes that contained premeasured volumes of recording buffer. The results shown in Fig. 4*B* represent data from 14 cells recorded from different culture plates with each cell serving as its own control. The sustained current was compared before and after galanin application at +20 mV, where this current is maximal. Slight inhibition was seen in 2 nM galanin and nearly complete inhibition was seen by 100–200 nM galanin. Results of these experiments are qualitative due to the method of galanin application and the accompanying uncertainty of whether the peptide is adsorbed to nonspecific binding sites in the cultures.

DISCUSSION

Insulin secretion, like neurotransmitter release, is known to be a calcium-dependent process (31). Glucose increases cytosolic free Ca^{2+} by several mechanisms, including depolarizing pancreatic β cells by decreasing K^+ conductance (26) and by directly enhancing Ca^{2+} entry through dihydropyridine-sensitive Ca^{2+} channels (32). The physiological regulation of insulin release involves a number of secretagogues and inhibitors of secretion, including the hormone glucagon, neurotransmitters, and neuromodulatory peptides such as somatostatin (26). Recent work on the pancreas had focused on neural influences on insulin release, and on galanin in particular, as a neurally released regulatory peptide that inhibits insulin release stimulated by traditional secretagogues such as glucose and arginine. Several mechanisms of action have been described for galanin. The inhibitory actions of galanin may be explained, in part, by direct hyperpolarization of the β-cell membranes caused by activating the ATP-dependent K^+ channels (33). As a result of this hyperpolarization, Ca^{2+} influx is reduced, causing a decrease in intracellular Ca^{2+} concentration, which in turn decreases insulin release. In the RIN cell line, galanin also hyperpolarizes the cell membrane, decreases intracellular Ca^{2+}, and inhibits basal and glyceraldehyde-stimulated insulin release (9).

Voltage-dependent Ca^{2+} channels have been observed in pancreatic β cells (24, 26–28) and in insulin-secreting cell lines (24, 34–36). Some studies on insulin-secreting cells (27, 28, 34–36), including this one, report evidence for two types of Ca^{2+} channels. Previous studies have provided evidence for great heterogeneity in the subclasses of voltage-gated Ca^{2+} channels (29), although they are often broadly described by the nomenclature of Nowycky *et al.* (37) as T-type, N-type, and L-type currents. With respect to RIN cells, the majority of the sustained Ca^{2+} current shares characteristics

common to L-type channels described in other preparations (29), including dihydropyridine-sensitivity. Galanin inhibits the sustained dihydropyridine-sensitive Ca^{2+} current in RIN cells but not the transient dihydropyridine-insensitive current.

The action of galanin on Ca^{2+} currents is likely to decrease insulin release under conditions where the cells are sufficiently depolarized. Glyceraldehyde stimulates the sustained Ca^{2+} current directly in voltage-clamped RIN cells (25). Thus, modulation of ion channels by galanin effectively inhibits insulin secretion in two ways: it overcomes membrane depolarization associated with K^+ channel inhibition by activating K^+ channels and it inhibits Ca^{2+} influx directly if the stimulus is strong enough to depolarize the cells above -30 mV and activate Ca^{2+} channels. Whether or not galanin inhibits dihydropyridine-sensitive Ca^{2+} currents in pancreatic β cells also may be a particularly important question with respect to regulation of glucose-stimulated insulin release since it was recently shown by Smith *et al.* (32) that glucose enhances activation of this Ca^{2+} current in pancreatic β cells. Feedback of synaptically released galanin onto presynaptic galanin receptors coupled to Ca^{2+} or K^+ channels in nerve terminals may be important mechanisms of galanin neuromodulatory control of insulin secretion *in vivo*.

The mechanism of galanin-mediated inhibition of dihydropyridine-sensitive Ca^{2+} currents is unknown. Several actions of galanin in RIN cells have been demonstrated to be pertussis toxin sensitive (9, 38, 39), including inhibition of adenylyl cyclase, inhibition of glyceraldehyde-stimulated insulin secretion, and the decrease in intracellular Ca^{2+} measured in intact Fura 2-loaded cells. If galanin's action to inhibit dihydropyridine-sensitive Ca^{2+} current in RIN cells follows parallels drawn from other neuropeptide and nonpeptide neurotransmitters, it too may be pertussis toxin sensitive (40). A recent report (41) suggested that where catecholamines were found to inhibit Ca^{2+} currents in another insulin-secreting cell line (HIT cells) through an α_2-adrenergic receptor a pertussis toxin-sensitive G-protein pathway was involved. Possible explanations for the diverse actions of galanin include multiple receptors for galanin, with each receptor mediating different cell functions, or one receptor for galanin with multiple mediators. Presently available data from galanin binding studies in RIN cell membranes indicate only one galanin receptor type in these cells (9, 39, 42).

We thank Dr. A. E. Boyd III for providing the RINm5f cells and Dr. C. R. Bliss for maintaining them. The work was supported in part by National Institutes of Health Grants NS24467, DK31667, and DK34305.

1. Tatemoto, K., Rokaeus, A., Jornvall, H., McDonald, T. J. & Mutt, V. (1983) *FEBS Lett.* **164,** 124–128.
2. Ch'ng, J. L. C., Christofides, N. D., Anand, P., Gibson, S. J., Allen, Y. S., Su, H. C., Tatemoto, K., Morrison, J. F. B., Polak, J. M. & Bloom, S. R. (1985) *Neuroscience* **16,** 343–354.
3. Ekblad, E., Rokaeus, A., Hakanson, R. & Sundler, F. (1985) *Neuroscience* **16,** 355–364.
4. Melander, T., Hokfelt, T., Rokaeus, A., Fakrenkrug, J., Tatemoto, K. & Mutt, V. (1985) *Cell Tissue Res.* **239,** 253–259.
5. Dunning, B. E., Ahren, B., Veith, R. C., Bottcher, G., Sundler, F. & Taborsky, G. J., Jr. (1986) *Am. J. Physiol.* **251,** E127–E133.
6. Hermansen, K. (1988) *Acta Endocrinol. (Copenhagen)* **119,** 91–98.
7. Nilsson, T., Arkhammar, P., Rorsman, P. & Berggren, P. O. (1989) *J. Biol. Chem.* **264,** 973–980.
8. Schnuerer, E. M., McDonald, T. J. & Dupre, J. (1987) *Regul. Pept.* **18,** 307–320.
9. Sharp, G. W. G., Le Marchand-Brustel, Y., Yada, T., Russo, L. L., Bliss, C. R., Cormont, M., Monge, L. & Van Obberghen, E. (1989) *J. Biol. Chem.* **264,** 7302–7309.
10. Silvestre, R. A., Miralles, P., Monge, L., Moreno, P., Villanueva, M. L. & Marco, J. (1987) *Endocrinology* **121,** 378–383.
11. Dunning, B. E. & Taborsky, G. J., Jr. (1989) *Am. J. Physiol.* **256,** E191–E198.
12. Yau, W. M., Dorsett, J. A. & Youther, M. L. (1986) *Neurosci. Lett.* **72,** 305–308.
13. Soldani, G., Mengozzi, G., Longa, A. D., Intorre, L., Martelli, F. & Brown, D. R. (1988) *Eur. J. Pharmacol.* **154,** 313–318.
14. Ottlecz, A., Snyder, G. D. & McCann, S. M. (1988) *Proc. Natl. Acad. Sci. USA* **85,** 9861–9865.
15. Tamura, K., Palmer, J. M., Winkelmann, C. K. & Wood, J. D. (1988) *J. Neurophysiol.* **60,** 966–979.
16. Konopka, L. M., McKeon, T. W. & Parsons, R. L. (1989) *J. Physiol. (London)* **410,** 107–122.
17. Ahren, B., Berggren, P. O., Bokvist, K. & Rorsman, P. (1989) *Peptides* **10,** 453–457.
18. de Weille, J. H., Fosset, M., Schmid-Antomarchi, H. & Lazdunski, M. (1989) *Brain Res.* **485,** 199–203.
19. Hamill, O. P., Marty, A., Neher, E., Sakmann, B. & Sigworth, F. J. (1981) *Pflügers Arch.* **391,** 85–100.
20. Forscher, P. & Oxford, G. S. (1985) *J. Gen. Physiol.* **85,** 743–763.
21. Horn, R. & Marty, A. (1988) *J. Gen. Physiol.* **92,** 145–159.
22. Findlay, I., Dunne, M. J. & Petersen, O. H. (1985) *J. Membr. Biol.* **88,** 165–172.
23. Rorsman, P., Arkhammar, P. & Berggren, P. O. (1986) *Am. J. Physiol.* **251,** C912–C919.
24. Findlay, I. & Dunne, M. J. (1985) *FEBS Lett.* **189,** 281–285.
25. Velasco, J. M., Petersen, J. U. H. & Petersen, O. H. (1988) *FEBS Lett.* **213,** 366–370.
26. Ashcroft, F. M., Kelly, R. P. & Smith, P. A. (1990) *Pflügers Arch.* **415,** 504–506.
27. Sala, S. & Matteson, D. R. (1990) *Biophys. J.* **58,** 567–571.
28. Rajan, A. S., Aguilar-Bryan, L., Nelson, D. A., Yaney, G. C., Hsu, W. H., Kunze, D. L. & Boyd, A. E., III (1990) *Diabetes Care* **13,** 340–363.
29. Bean, B. P. (1989) *Annu. Rev. Physiol.* **51,** 367–384.
30. Simasko, S. M., Weiland, G. A. & Oswald, R. E. (1988) *Am. J. Physiol.* **254,** E328–E336.
31. Wollheim, C. B. & Sharp, G. W. G. (1981) *Physiol. Rev.* **61,** 914–973.
32. Smith, P. A., Rorsman, P. & Ashcroft, F. M. (1989) *Nature (London)* **342,** 550–553.
33. de Weille, J. H., Schmid-Antomarchi, H., Fosset, M. & Lazdunski, M. (1988) *Proc. Natl. Acad. Sci. USA* **85,** 1312–1316.
34. Satin, L. S. & Cook, D. L. (1988) *Pflügers Arch.* **411,** 401–409.
35. Hiriart, M. & Matteson, D. R. (1987) *J. Gen. Physiol.* **91,** 617–639.
36. Komatsu, M., Yokokawa, N., Takeda, T., Nagasawa, Y., Aizawa, T. & Yamada, T. (1989) *Endocrinology* **125,** 2008–2014.
37. Nowycky, M. C., Fox, A. P. & Tsien, R. W. (1985) *Nature (London)* **316,** 440–442.
38. Amiranoff, B., Lorinet, A. M., Lagney-Pourmir, I. & Laburthe, M. (1988) *Eur. J. Biochem.* **177,** 147–152.
39. Lagny-Pourmir, I., Amiranoff, B., Lorinet, A. M., Tatemoto, K. & Laburthe, M. (1989) *Endocrinology* **124,** 2635–2641.
40. Nicoll, R. A., Malenka, R. C. & Kauer, J. A. (1990) *Physiol. Rev.* **70,** 513–565.
41. Keahey, H. H., Boyd, A. E., III, & Kunze, D. L. (1989) *Am. J. Physiol.* **257,** C1171–C1176.
42. Amiranoff, B., Lorinet, A. M. & Laburthe, M. (1989) *J. Biol. Chem.* **264,** 20714–20717.